



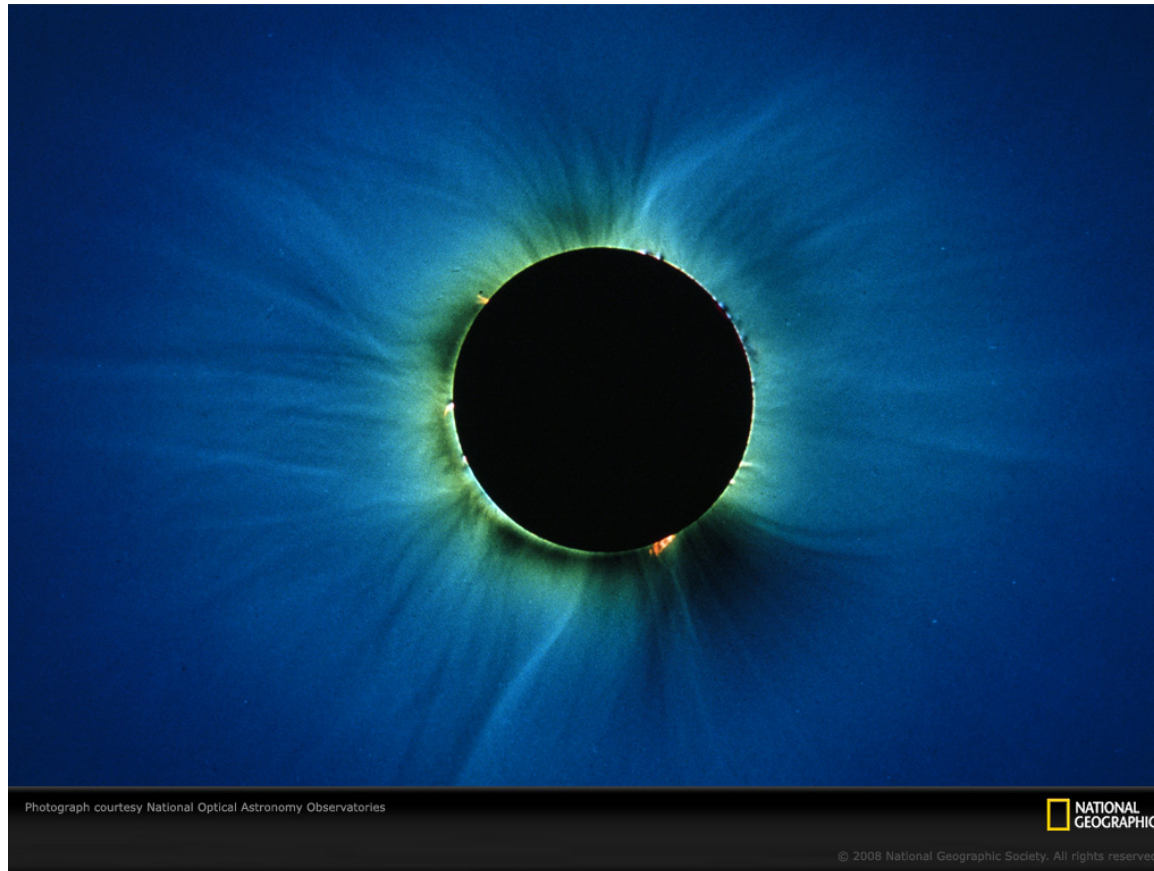
AARHUS
UNIVERSITET

Stellar activity I

CHRISTOFFER KAROFF

VERSITET

WHAT IS STELLAR ACTIVITY?

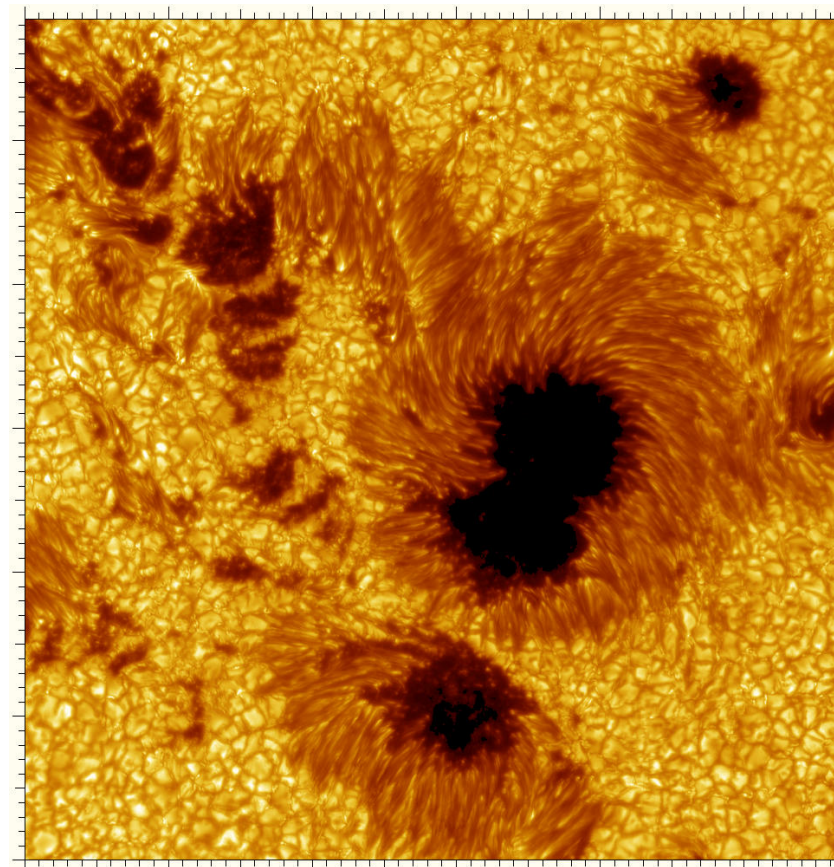


Photograph courtesy National Optical Astronomy Observatories

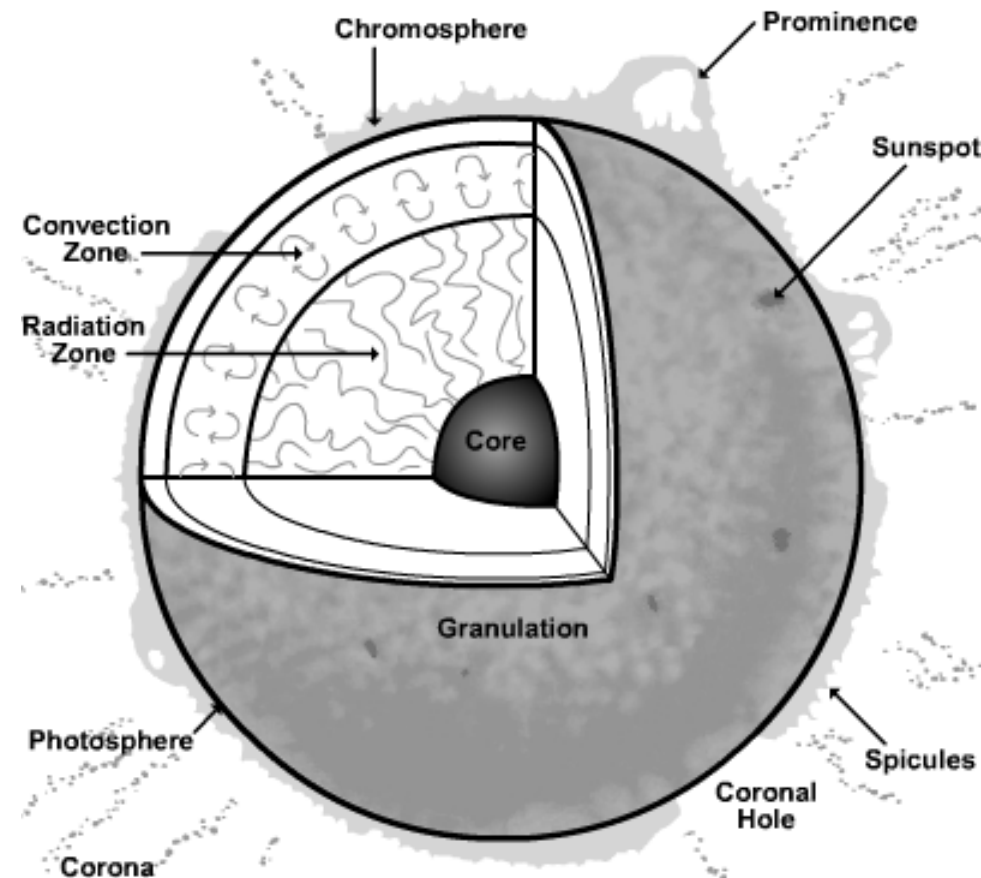
NATIONAL
GEOGRAPHIC

© 2008 National Geographic Society. All rights reserved.

WHAT IS STELLAR ACTIVITY?



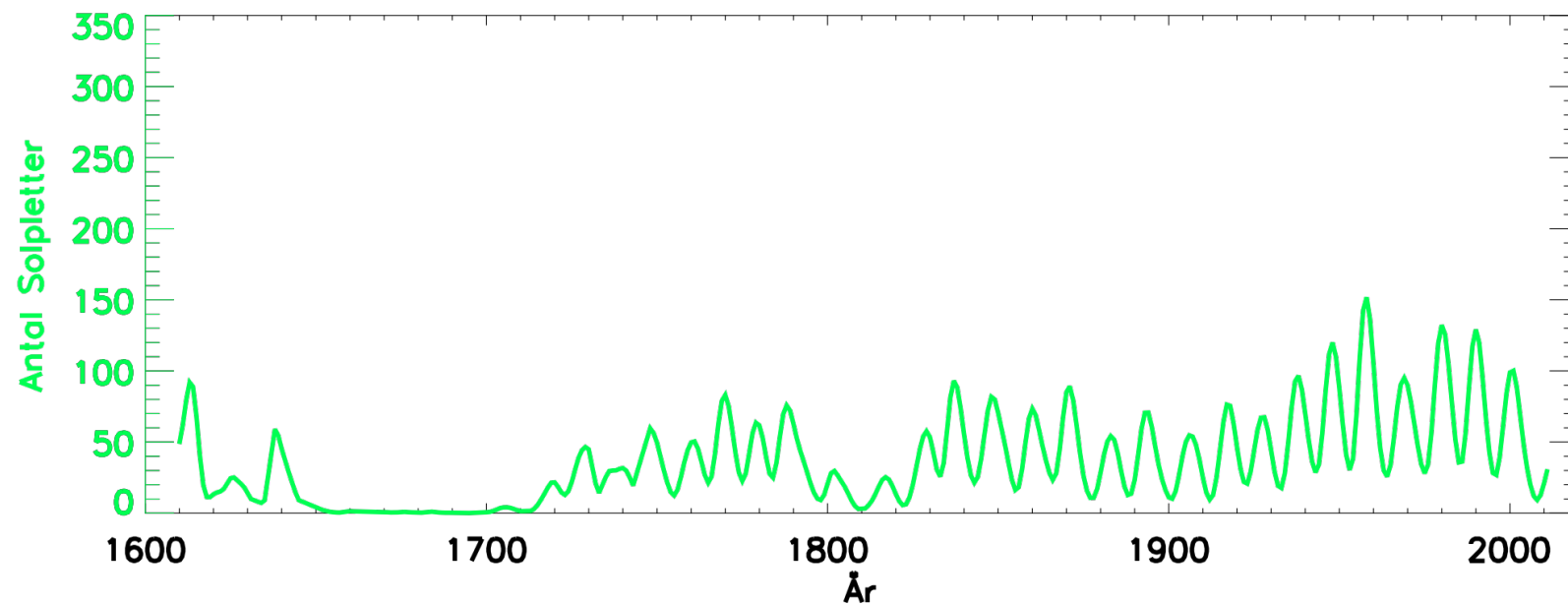
ACTIVITY ON SUN-LIKE STARS



WAYS TO MEASURE SOLAR STELLAR ACTIVITY

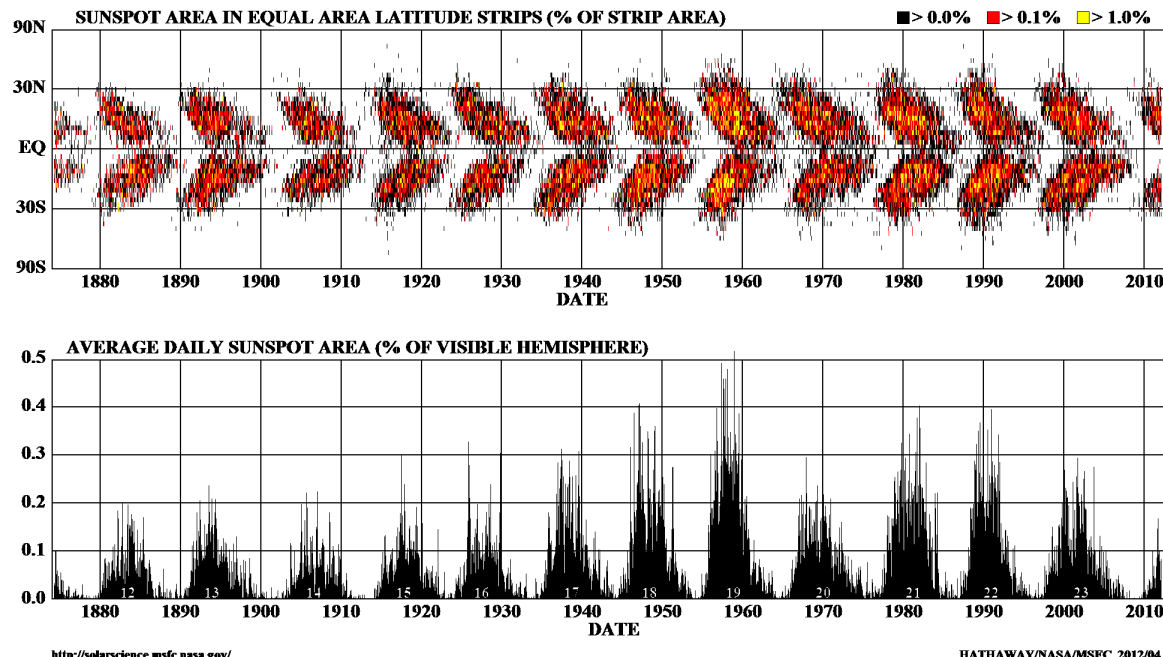
- › Sun spots
- › Plage
- › Amplitude, frequency and lifetime of p (and g!!!)-mode oscillations
- › Facular
- › Flares
- › X-rays

THE SOLAR CYCLE



BUTTERFLY DIAGRAM

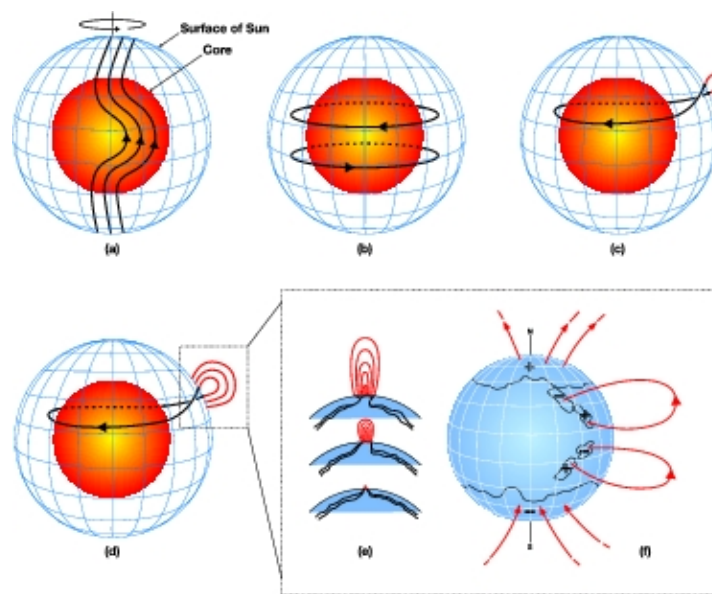
DAILY SUNSPOT AREA AVERAGED OVER INDIVIDUAL SOLAR ROTATIONS



<http://solarscience.msfc.nasa.gov/>

HATHAWAY/NASA/MSFC 2012/04

THE SOLAR DYNAMO

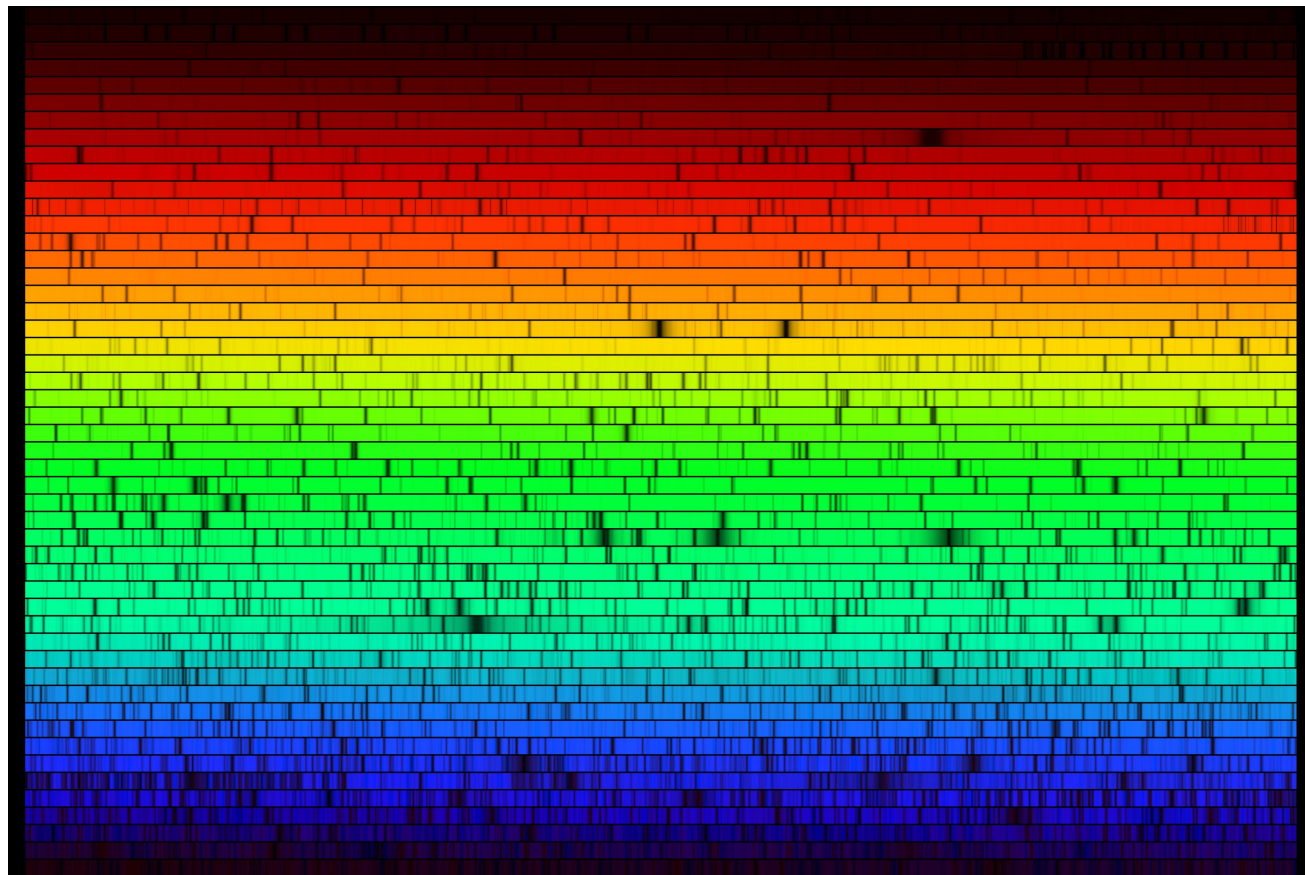


The solar cycle is caused by the solar dynamo.

The solar dynamo consists of the Ω and α -effects.

Ω and α -effects are driven by the differential rotation of the Sun and by convection.

HOW TO MEASURE ACTIVITY ON SUN-LIKE STARS



HOW TO MEASURE ACTIVITY ON SUN-LIKE STARS

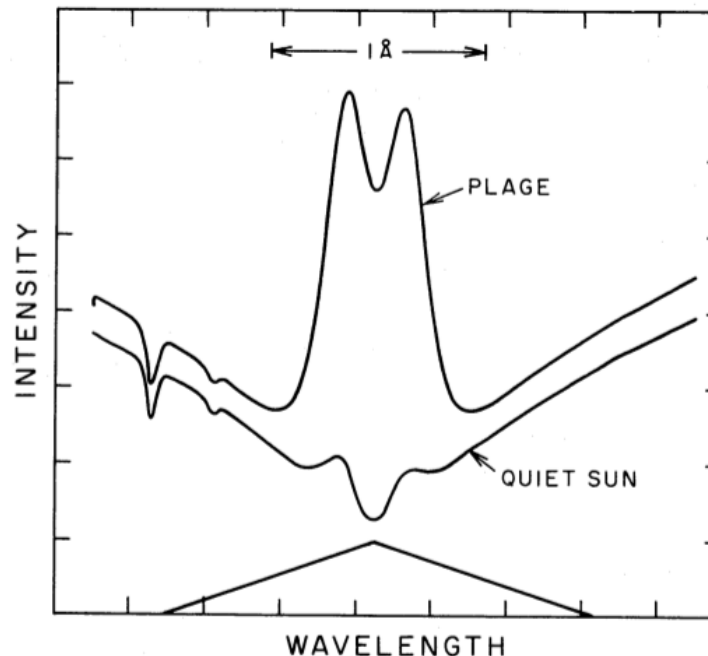
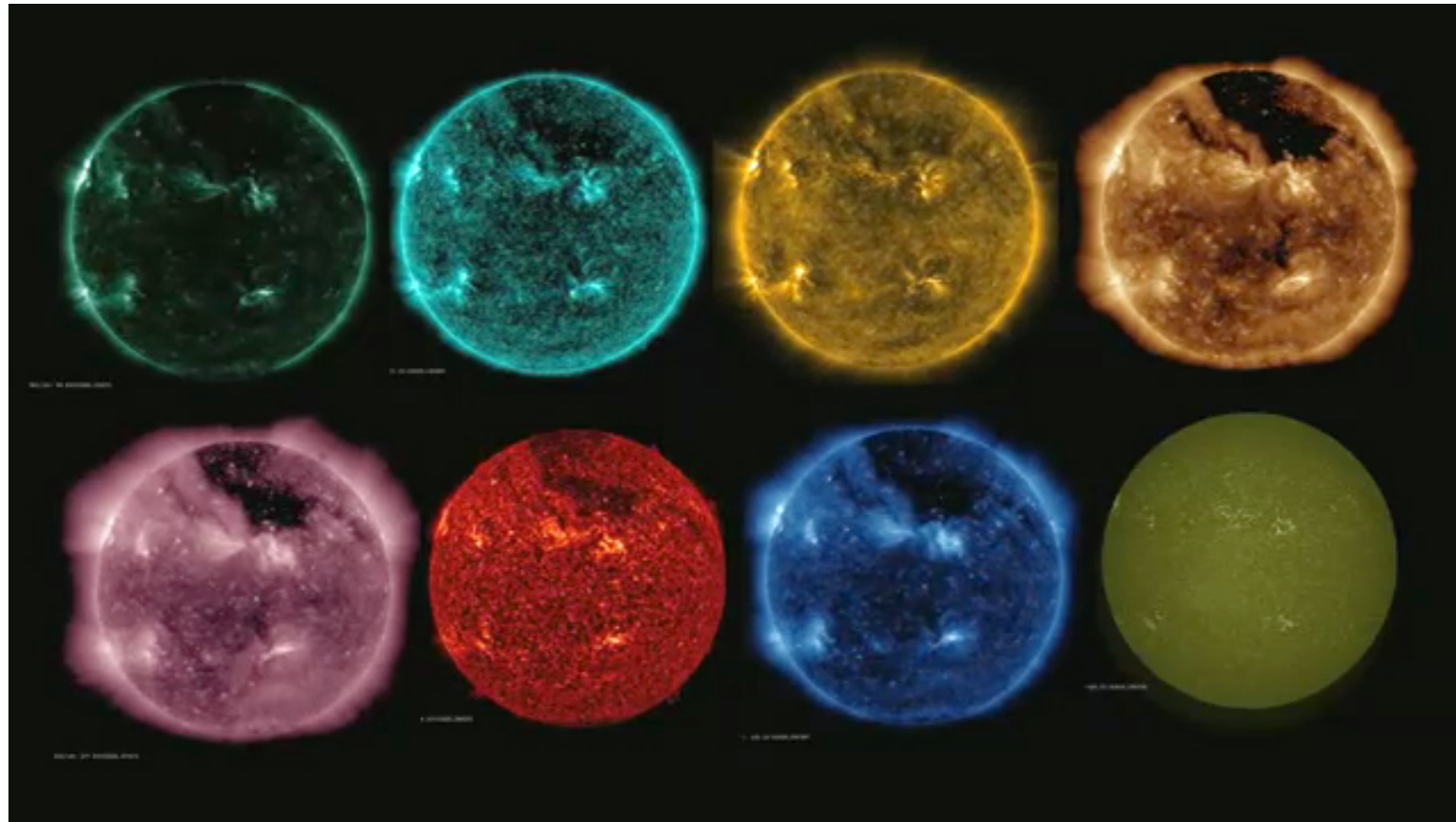
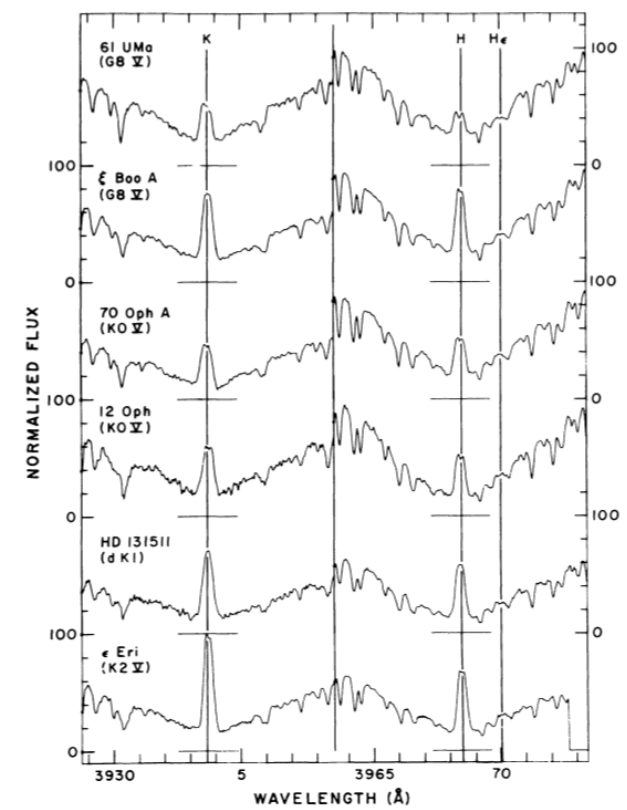
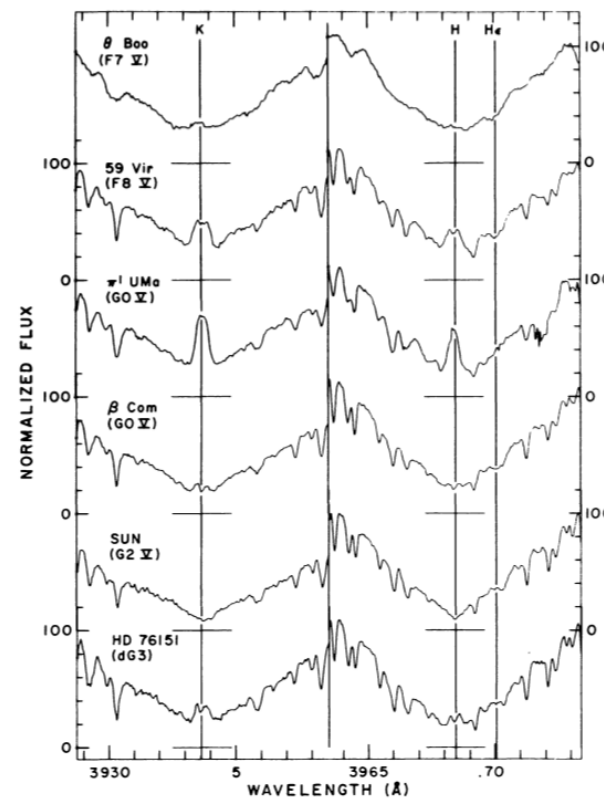
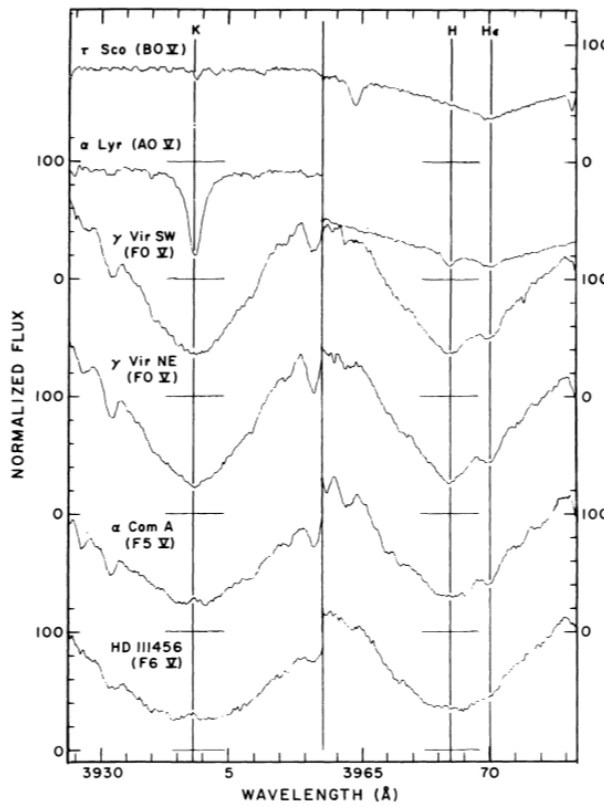


FIG. 1.—The solar Ca II K line profile at different levels of activity. The triangle shows the effective transmission profile of the Mount Wilson HK spectrophotometer (adapted from White and Livingstone 1981).

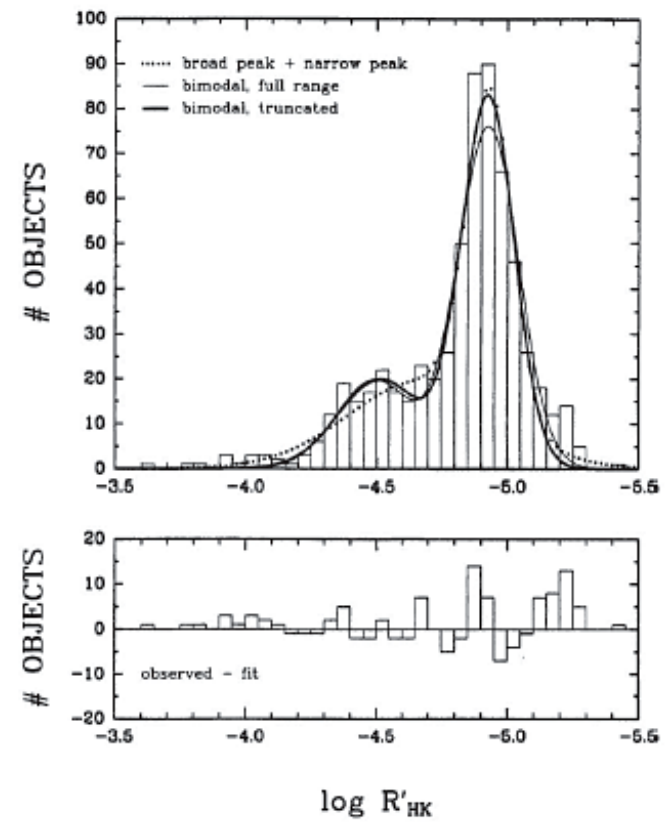
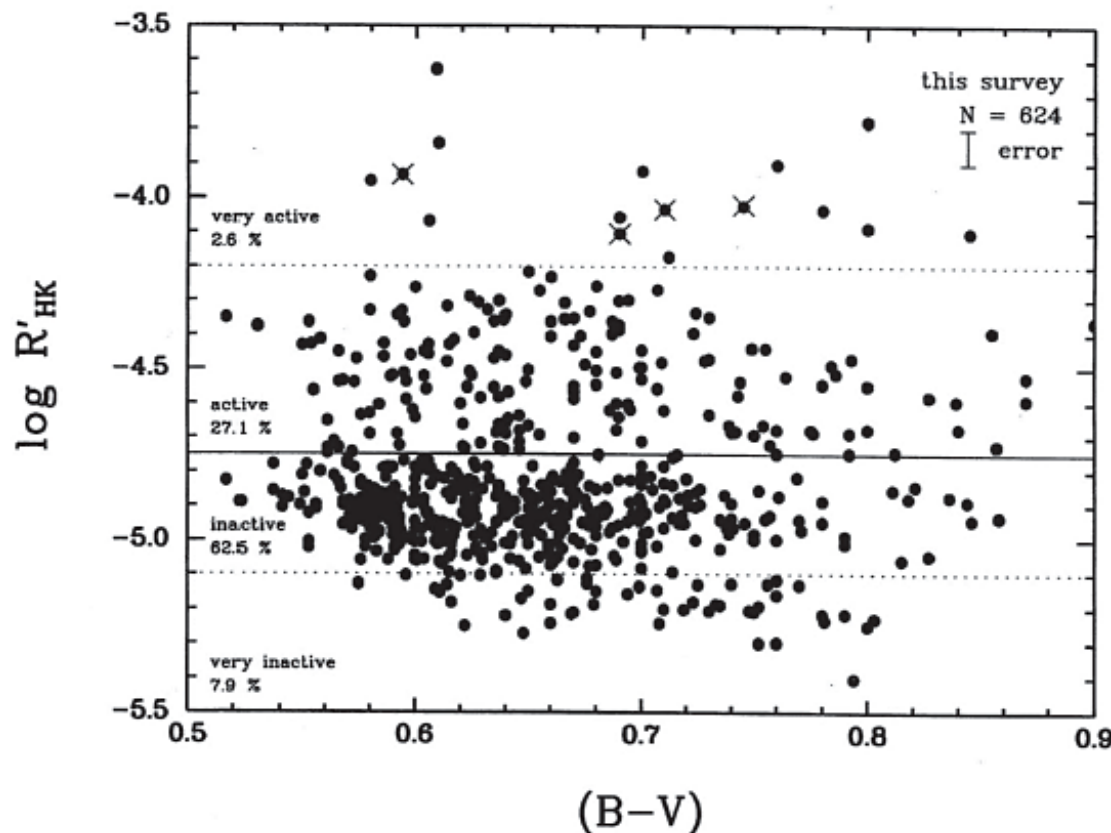
PLAGE



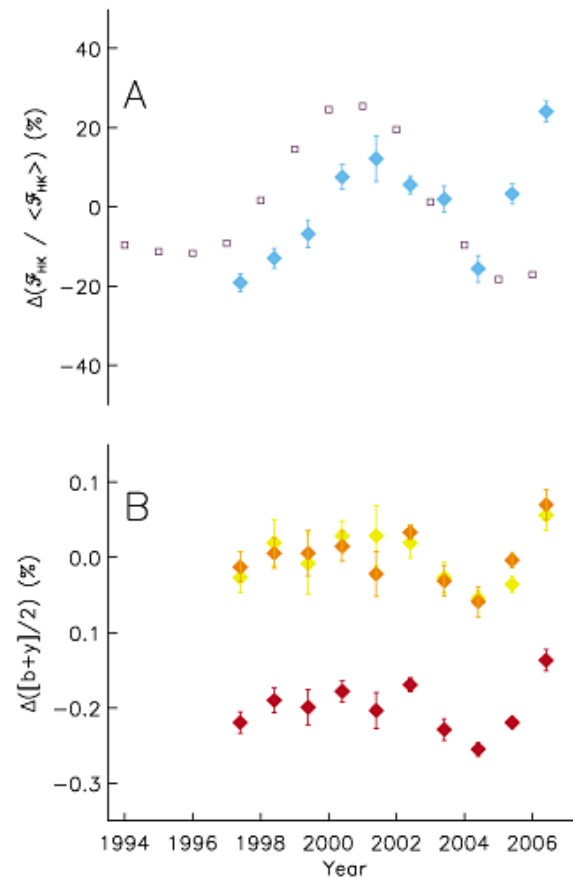
STELLAR ACTIVITY



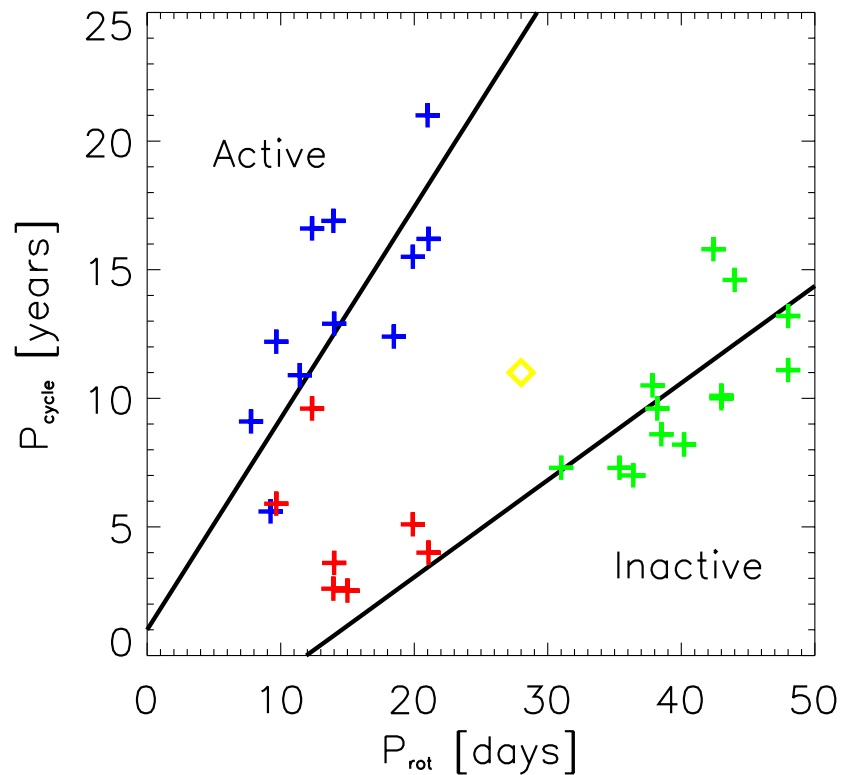
DISTRIBUTION OF STELLAR ACTIVITY



18 SCORPIL



THE BÖHM-VITENSE HYPOTHESIS



1.6 Y CYCLE IN ι HOROLOGII

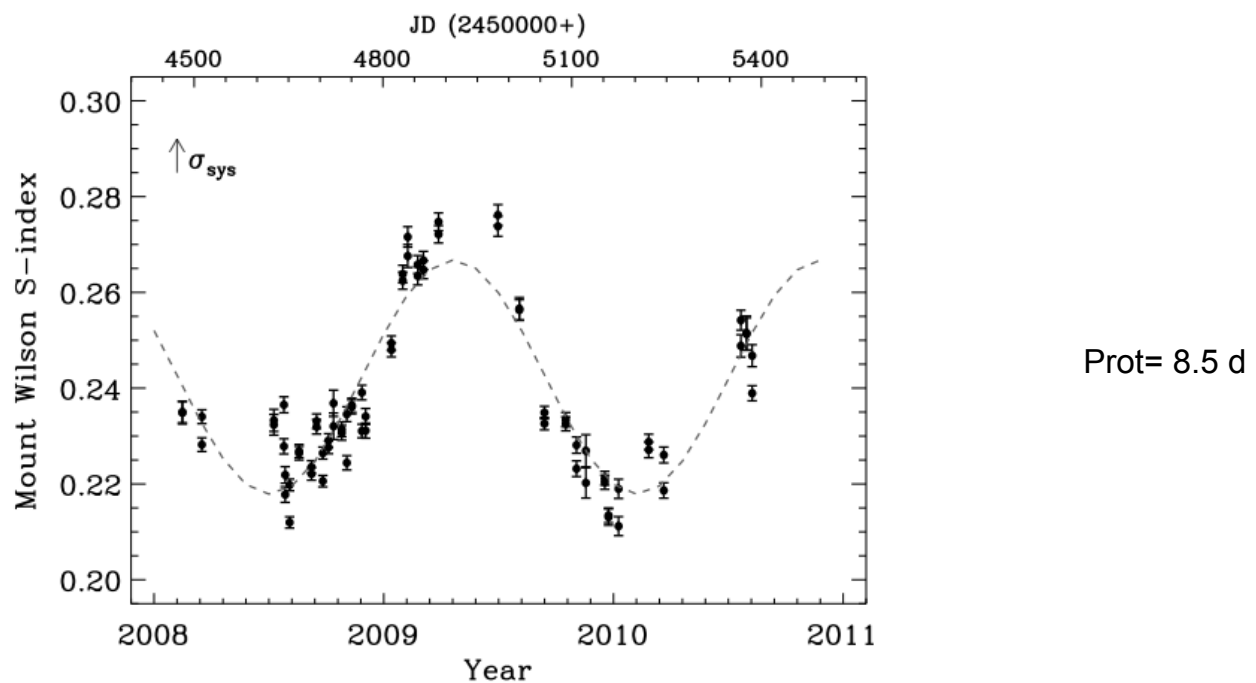


Figure 1. Chromospheric activity measurements of the F8V star ι Hor from the southern HK survey (Metcalfe et al. 2009), showing a clear variation with a cycle period of 1.6 years, the shortest cycle measured for a Sun-like star. Note that the error bars represent only the measurement errors and do not include the systematic uncertainty $\sigma_{\text{sys}} \sim 0.007$ (arrow).

~120 D CYCLE IN HD 49933

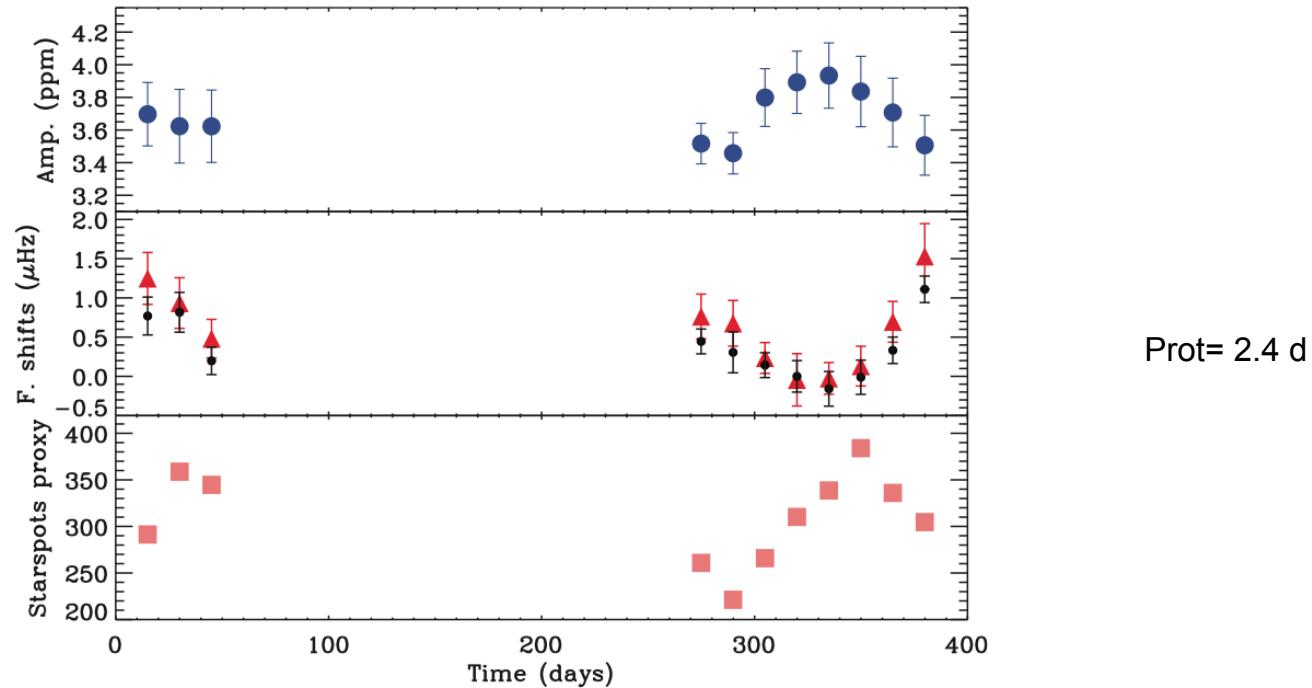


Fig. 1. Time evolution beginning 6 February 2007 of the mode amplitude (**top**); the frequency shifts using two different methods (**middle**), cross correlations (red triangles) and individual frequency shifts (black circles); and a starspot proxy (**bottom**) built by computing the standard deviation of the light curve (7). All of them were computed by using 30-day-long subseries shifted every 15 days (50% overlapping). The corresponding 1σ error bars are shown.

AND THE SUN

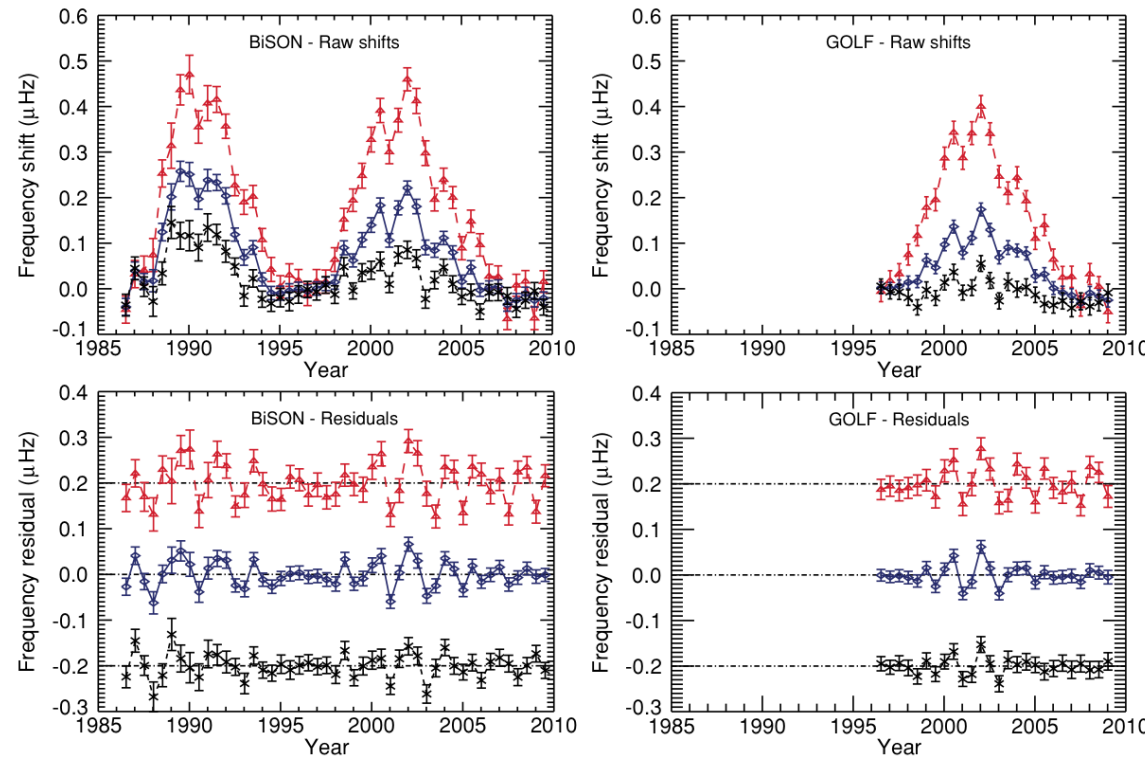


Figure 1. Top: average frequency shifts of “Sun-as-a-star” modes with frequencies between 1.88 and 3.71 mHz (total-frequency band, blue solid line, and diamond symbols); 1.88 and 2.77 mHz (low-frequency band, black dotted line, and cross symbols); and 2.82 and 3.71 mHz (high-frequency band, red dashed line, and triangle symbols). Bottom: residuals left after dominant 11 year signal has been removed (black dotted and red dashed curves are displaced by -0.2 and $+0.2$, respectively, for clarity).

DEFINITION OF CHROMOSPHERIC FLUX

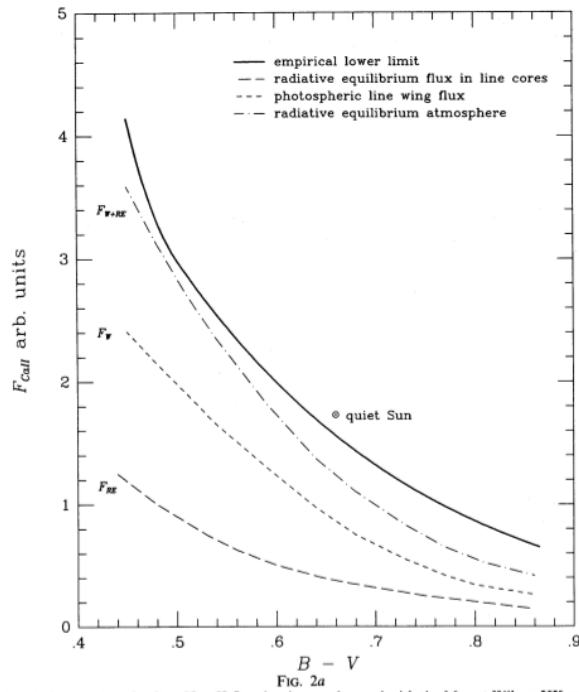


FIG. 2.—(a–c) The three panels in this figure relate the Ca II H + K flux density, as observed with the Mount Wilson HK spectrophotometer, to $B - V$ color. The empirical lower-limit flux (§ IIa) is shown in each of the panels to provide a common reference. In addition (a) shows the observed photospheric flux in the line wings (§ IIc), the computed radiative-equilibrium flux in the line cores (§ IIc), and the total flux expected from an atmosphere in radiative equilibrium; (b) shows typical fluxes observed for the Sun (§ IIb), the Ca II H + K flux to be subtracted for the maximum correlation with X-ray emission (§ IIe), and the Mg II $h + k$ lower limit flux (§ IIa), converted to an equivalent Ca II H + K flux; (c) shows the intercept $a_0(B - V)$ (§ IIIa) of the relation between Ca II H + K and Mg II $h + k$ fluxes, and the intercepts of the activity-variability (§ IIIb) and the rotation-activity (§ IIIc) relations.

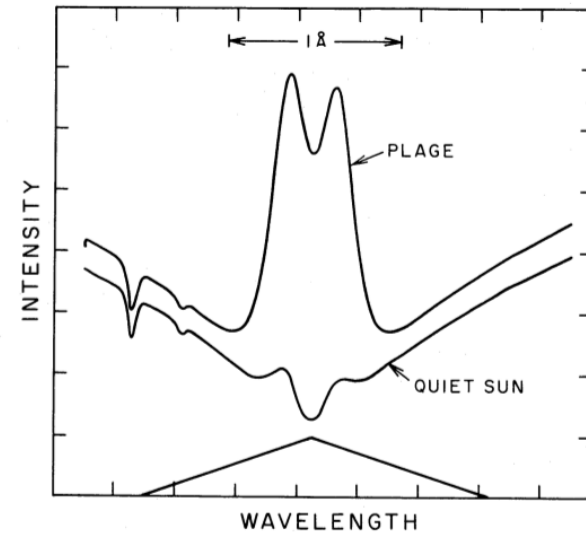
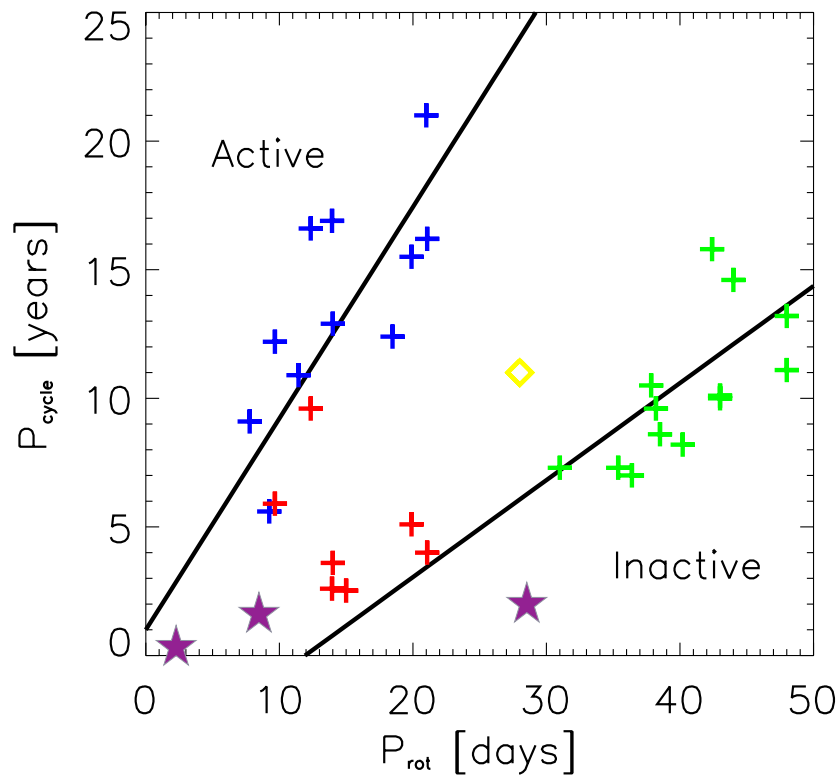


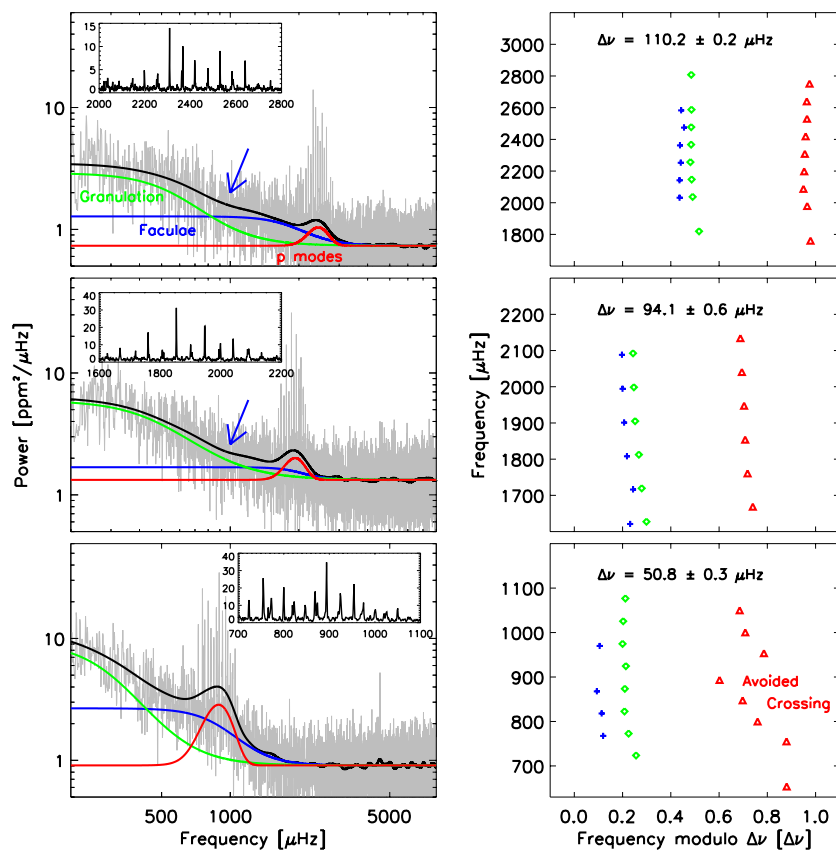
FIG. 1.—The solar Ca II K line profile at different levels of activity. The triangle shows the effective transmission profile of the Mount Wilson HK spectrophotometer (adapted from White and Livingstone 1981).

THE BÖHM-VITENSE HYPOTHESIS



- Active stars have ~ 300 rotations per cycle
- Inactive stars have ~ 100
- I Horologii has 70
- HD 49933 has 50
- 2nd Sun has 30

ASTEROSEISMOLOGY WITH KEPLER



WAYS TO MEASURE SOLAR STELLAR ACTIVITY

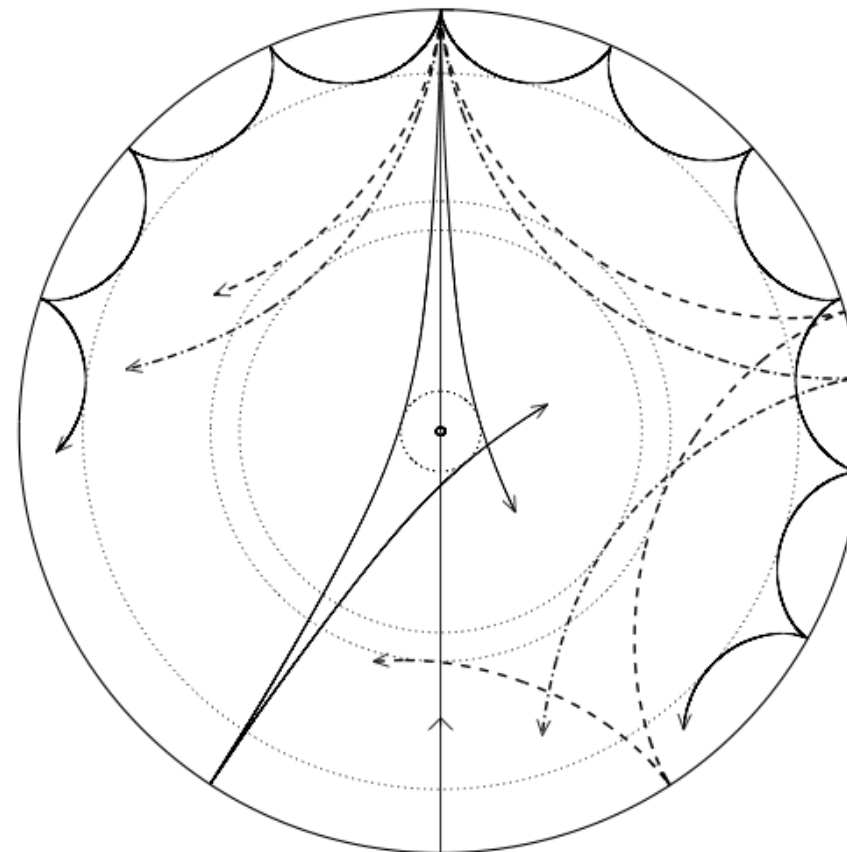
- › Sun spots
- › Plage
- › Amplitude, frequency and lifetime of p (and g!!!)-mode oscillations
- › Facular
- › Flares
- › X-rays

WHY ARE G-MODES SO INTERESTING?



STELLAR ASTROPHYSICS CENTRE

WHY ARE G-MODES SO INTERESTING?



WHY ARE G-MODES SO INTERESTING?

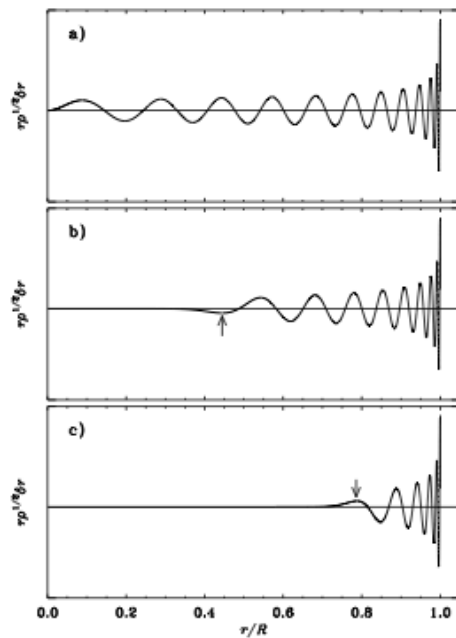


Figure 5.8: Scaled radial displacement eigenfunctions for selected p modes in a normal solar model, with a) $l = 0$, $n = 23$, $\nu = 3310 \mu\text{Hz}$; b) $l = 20$, $n = 17$, $\nu = 3375 \mu\text{Hz}$; c) $l = 60$, $n = 10$, $\nu = 3234 \mu\text{Hz}$. The arrows mark the asymptotic location of the turning points r_t [cf. equation (5.28)].

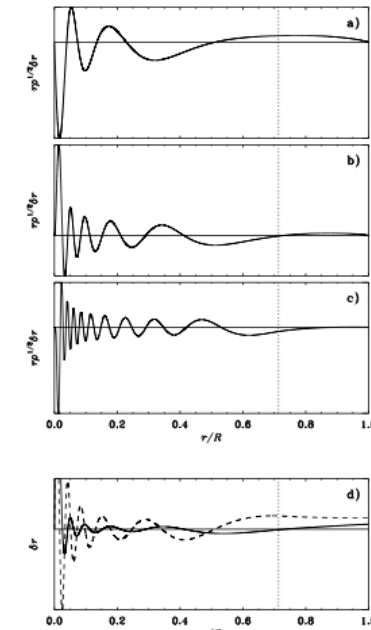
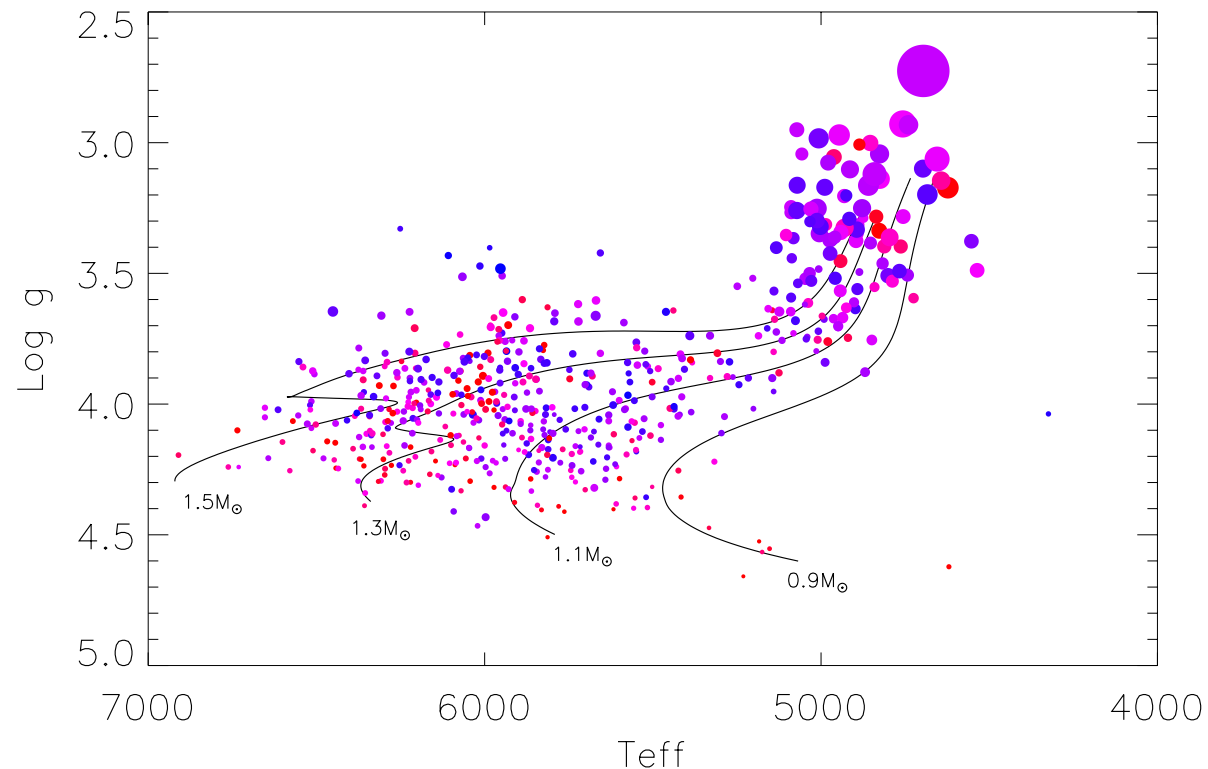
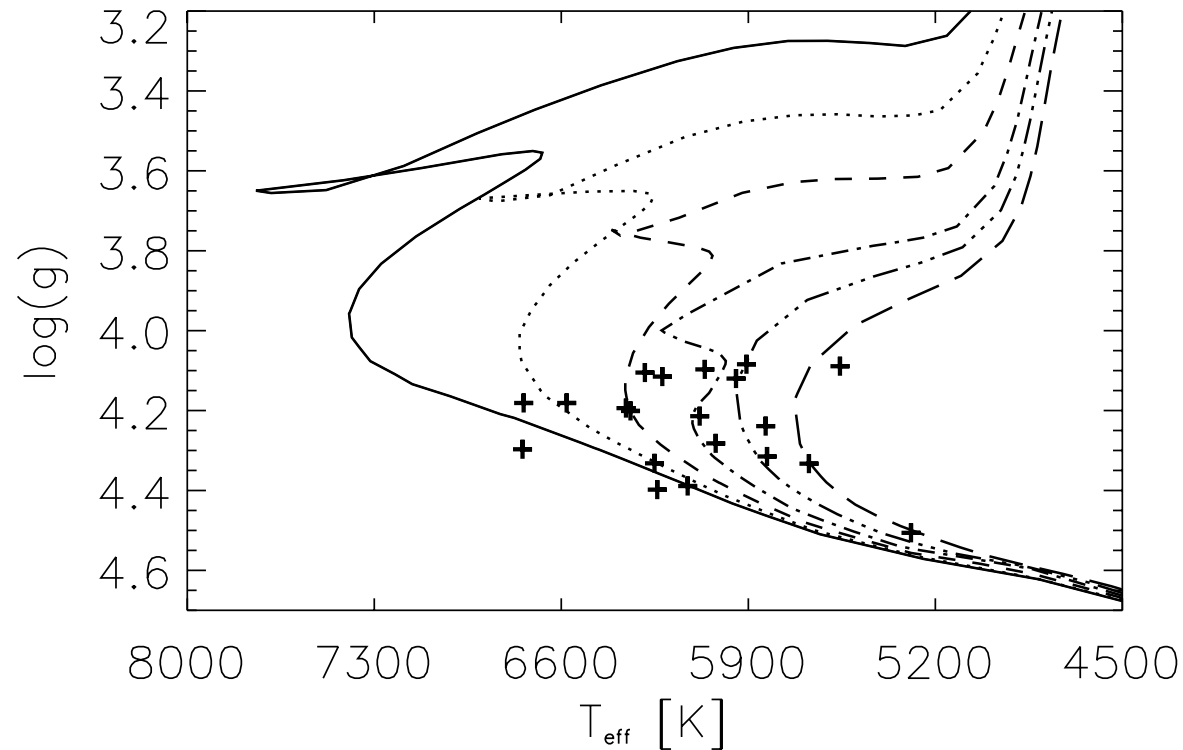


Figure 5.10: Eigenfunctions for selected g modes in a normal solar model. Panels a) to c) show scaled radial displacement eigenfunctions with a) $l = 1$, $n = -5$, $\nu = 110 \mu\text{Hz}$; b) $l = 2$, $n = -10$, $\nu = 103 \mu\text{Hz}$; c) $l = 4$, $n = -19$, $\nu = 100 \mu\text{Hz}$. In panel d) the solid and dashed curves show unscaled radial (ξ_r) and horizontal displacement ($L\xi_l$) eigenfunctions, for the $l = 2$, $n = -10$ mode. For clarity, the curve for ξ_r has been truncated: the maximum value is about 2.7 times higher than the largest value shown. The vertical dotted line marks the base of the convective envelope.

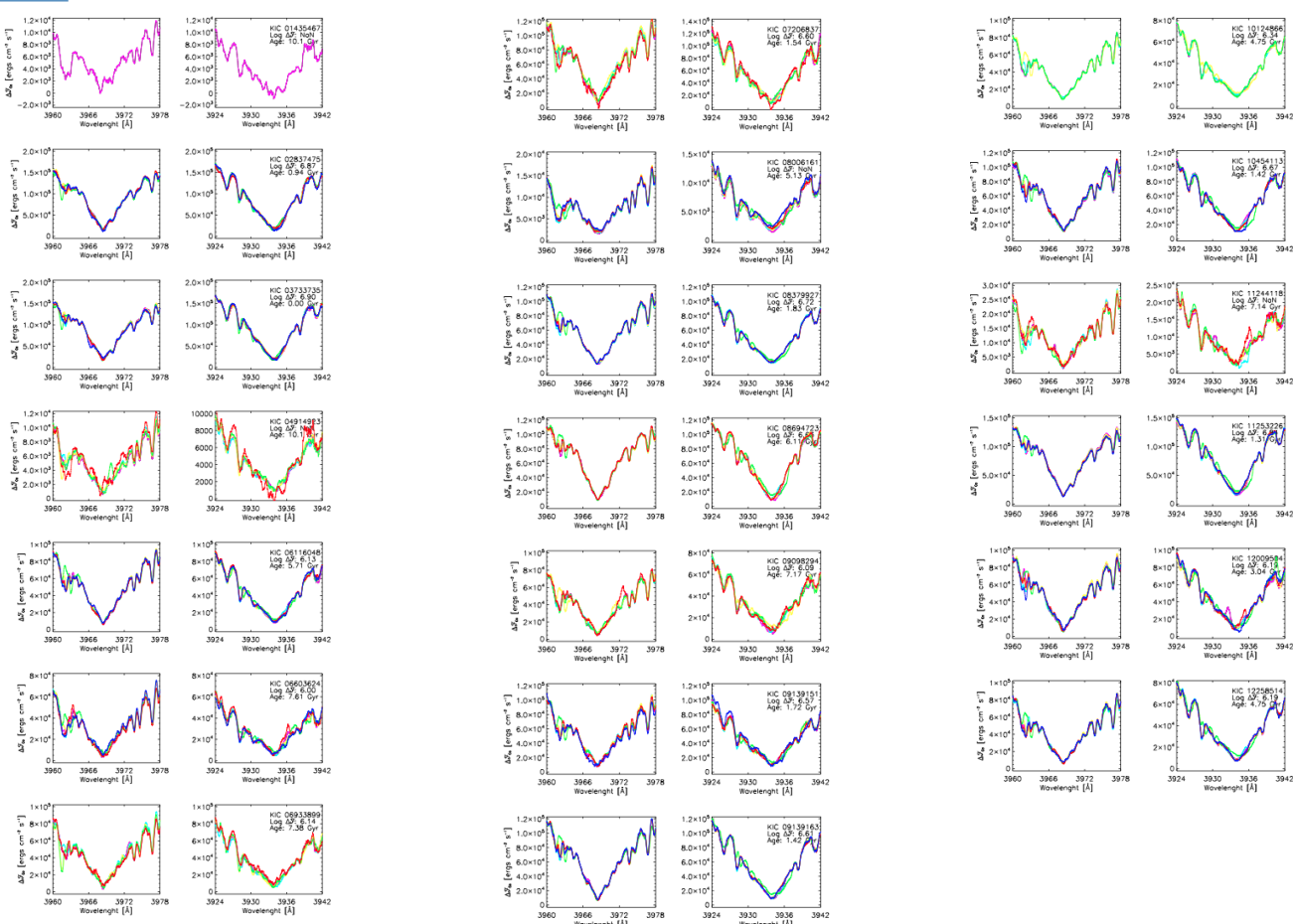
LIMIT NUMBER OF COOL STARS...



THE 20 MOST SUN-LIKE STARS



THE 20 MOST SUN-LIKE STARS



DEFINITION OF CHROMOSPHERIC FLUX

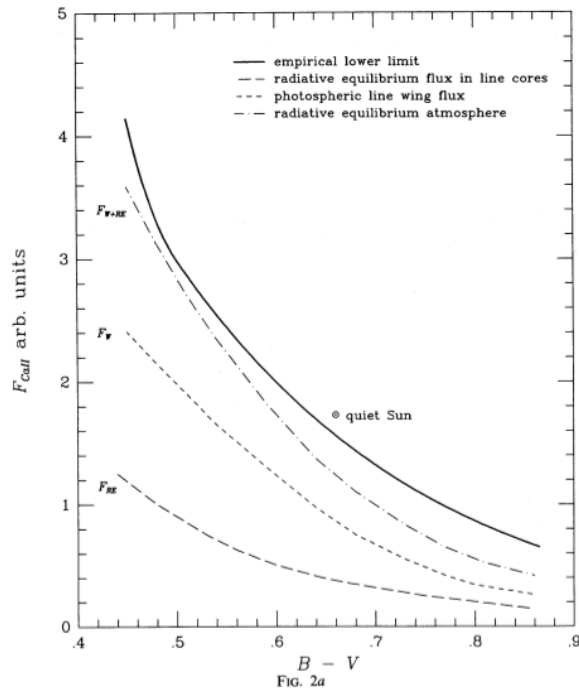


FIG. 2.—(a–c) The three panels in this figure relate the Ca II H + K flux density, as observed with the Mount Wilson HK spectrophotometer, to $B - V$ color. The empirical lower-limit flux (§ IIa) is shown in each of the panels to provide a common reference. In addition (a) shows the observed photospheric flux in the line wings (§ IIc), the computed radiative-equilibrium flux in the line cores (§ IIc), and the total flux expected from an atmosphere in radiative equilibrium; (b) shows typical fluxes observed for the Sun (§ IIb), the Ca II H + K flux to be subtracted for the maximum correlation with X-ray emission (§ IIe), and the Mg II $h + k$ lower limit flux (§ IIa), converted to an equivalent Ca II H + K flux; (c) shows the intercept $a_0(B - V)$ (§ IIIa) of the relation between Ca II H + K and Mg II $h + k$ fluxes, and the intercepts of the activity-variability (§ IIIb) and the rotation-activity (§ IIIc) relations.

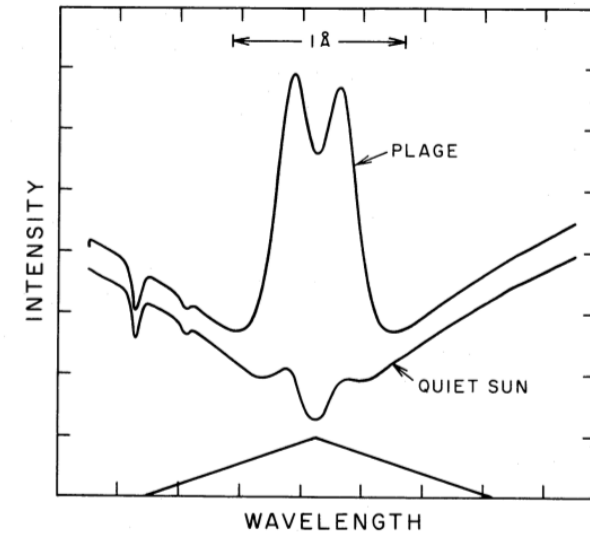


FIG. 1.—The solar Ca II K line profile at different levels of activity. The triangle shows the effective transmission profile of the Mount Wilson HK spectrophotometer (adapted from White and Livingstone 1981).

ACTIVITY-AGE-ROTATION RELATIONS

THE ASTROPHYSICAL JOURNAL, 171:565–567, 1972 February 1
 © 1972. The University of Chicago All rights reserved. Printed in U S A

TIME SCALES FOR Ca II EMISSION DECAY, ROTATIONAL BRAKING, AND LITHIUM DEPLETION

A. SKUMANICH

High Altitude Observatory, National Center for Atmospheric Research,* Boulder, Colorado

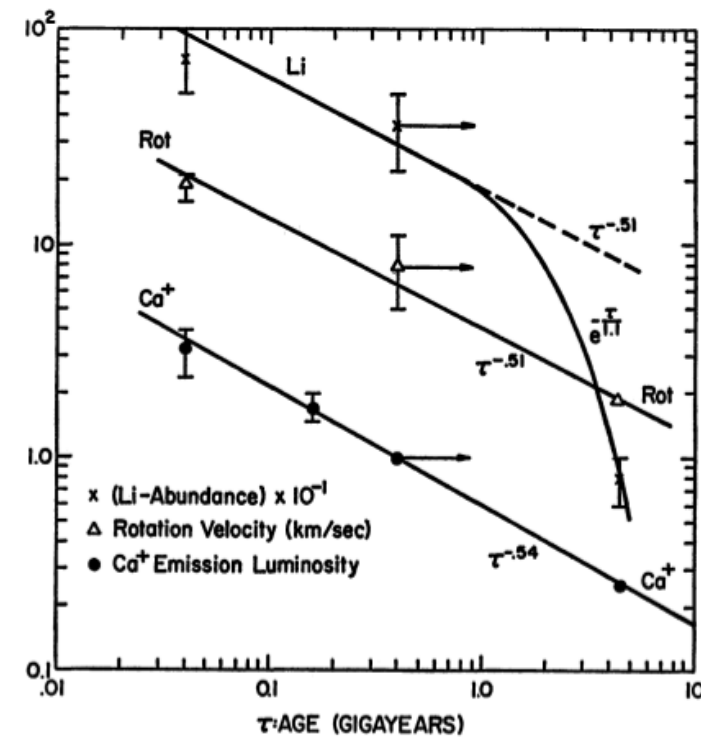
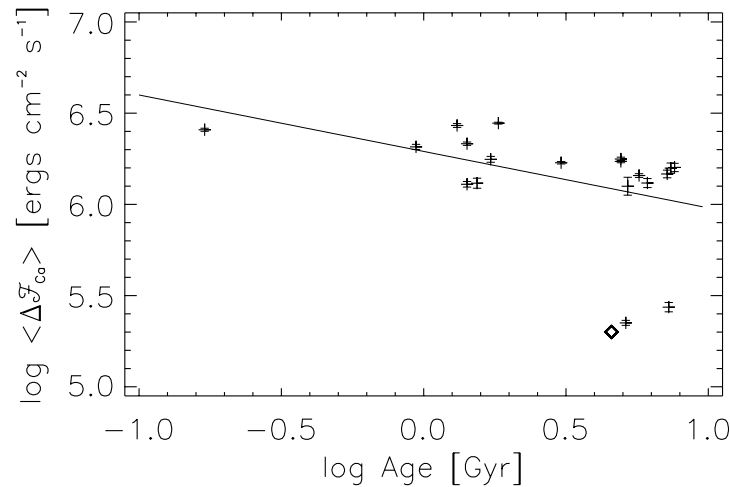
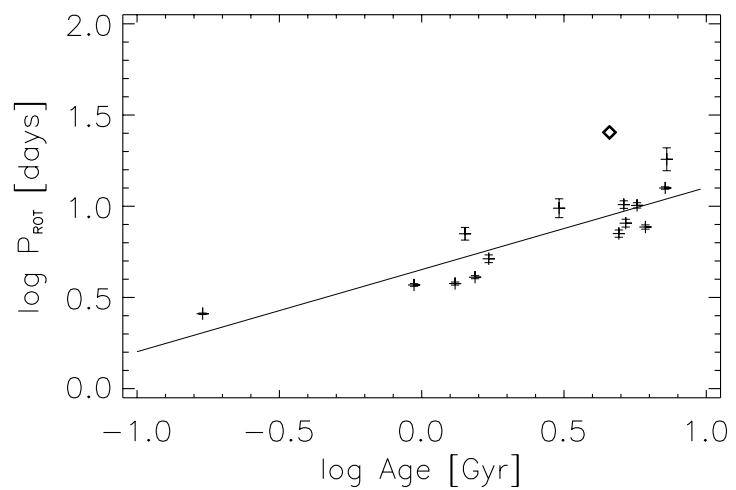
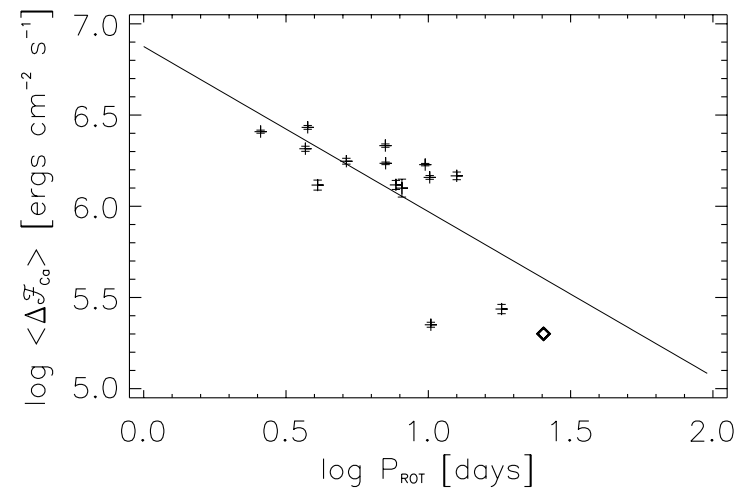
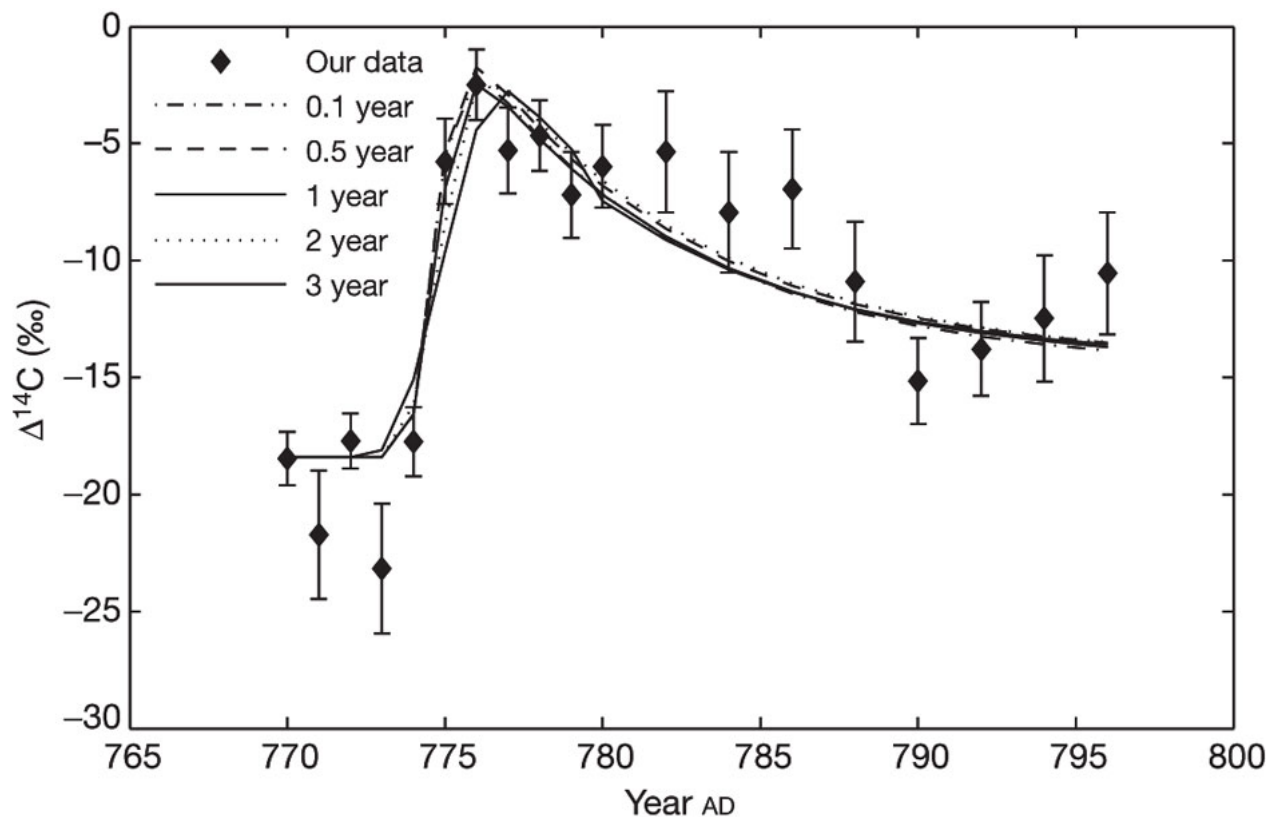


FIG. 1.—Ca⁺ emission, rotation, and lithium abundance versus stellar age

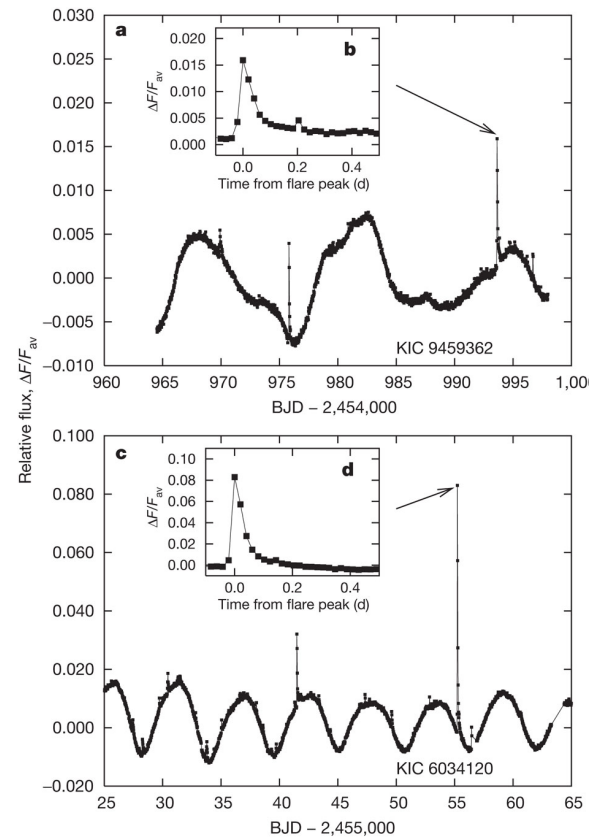
ACTIVITY-AGE-ROTATION RELATIONS



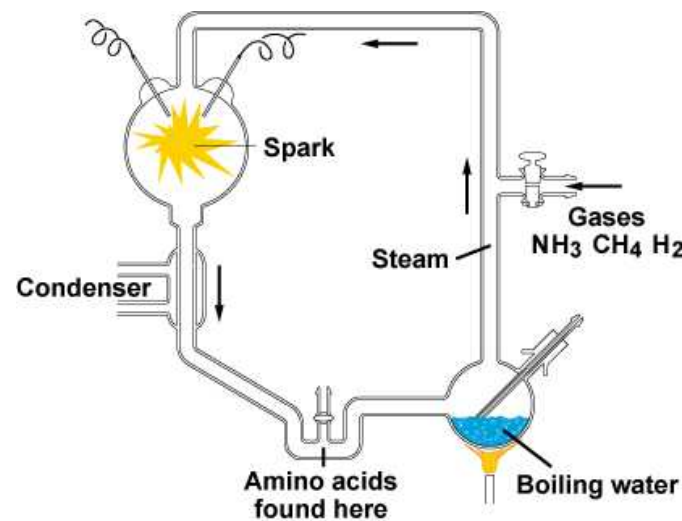
COSMIC-RAY INCREASE IN AD 774-775

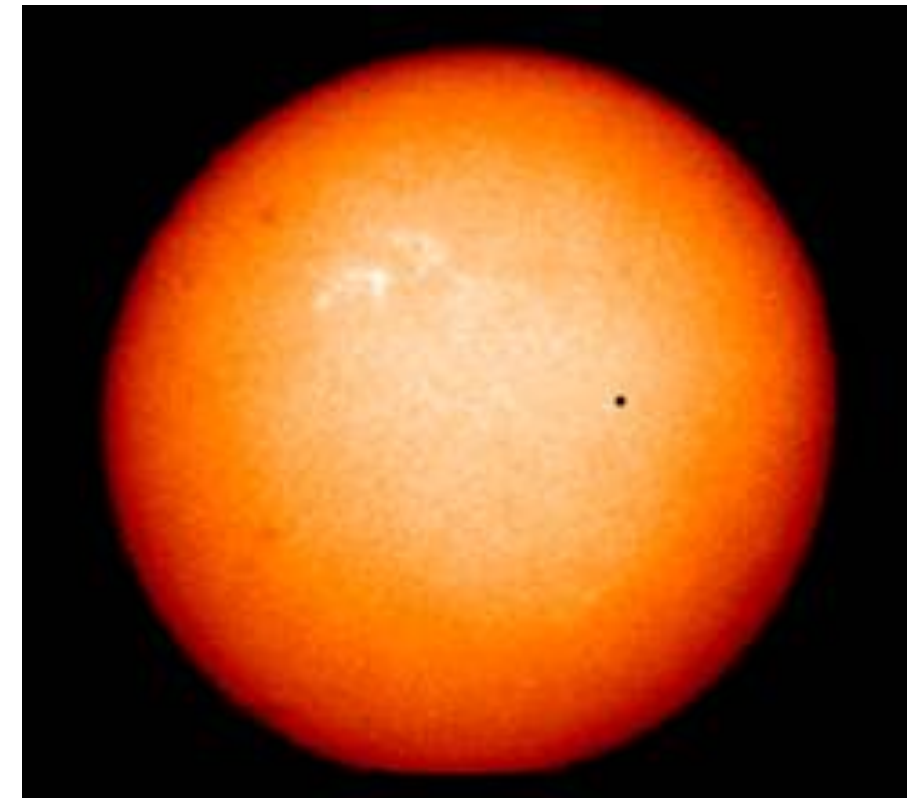
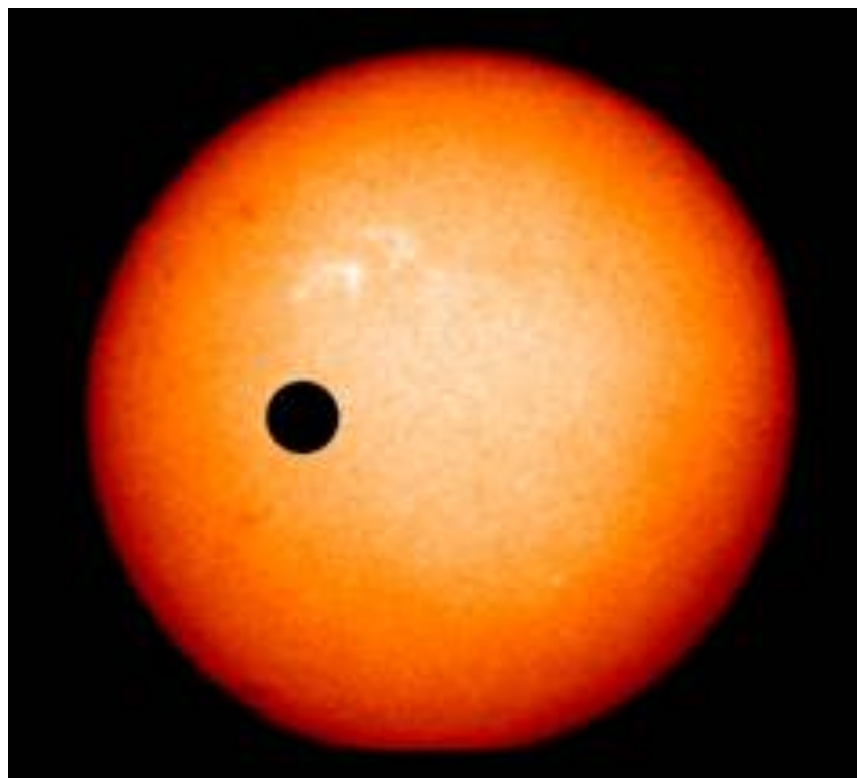


SUPERFLARES ON SOLAR-TYPE STARS

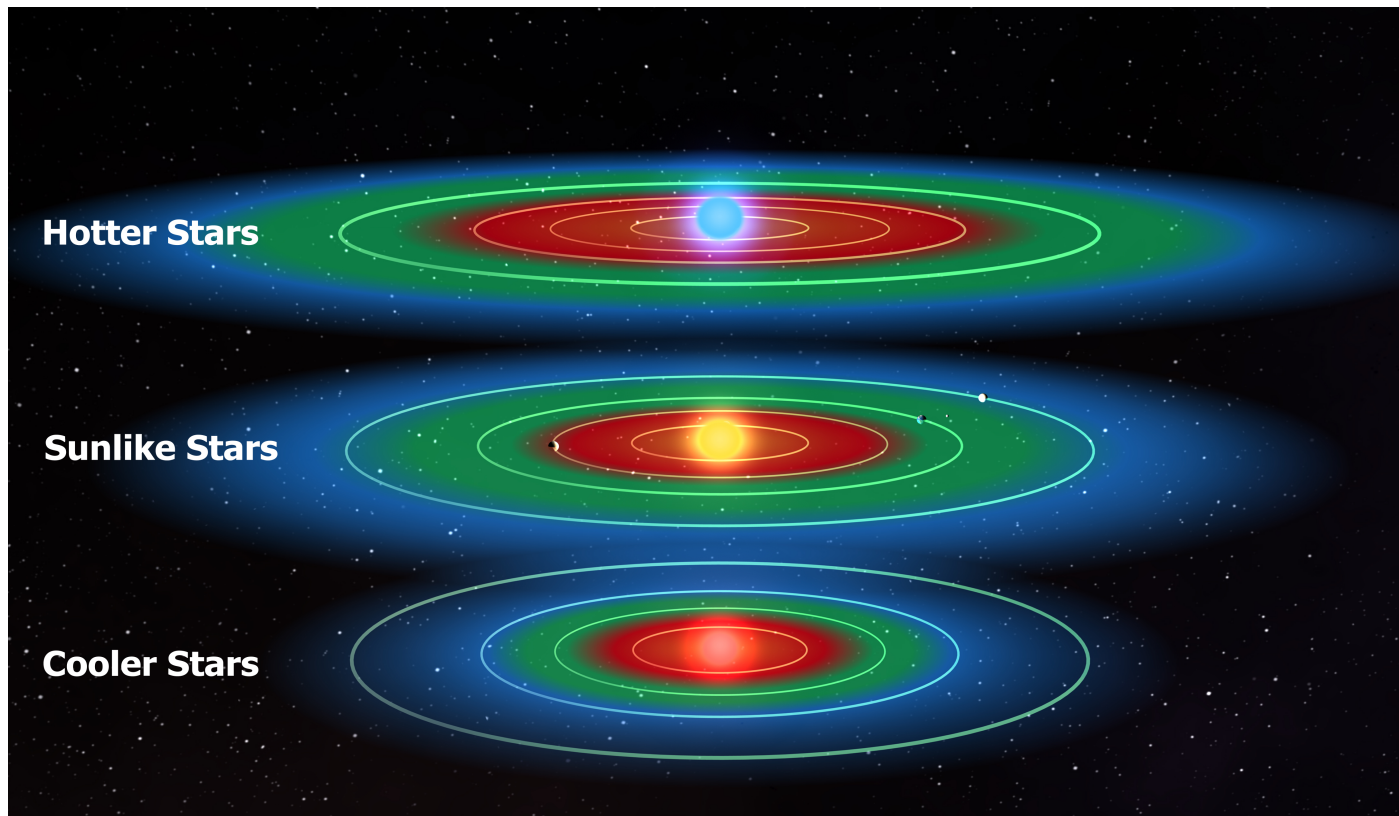


THE MILLER-UREY EXPERIMENT

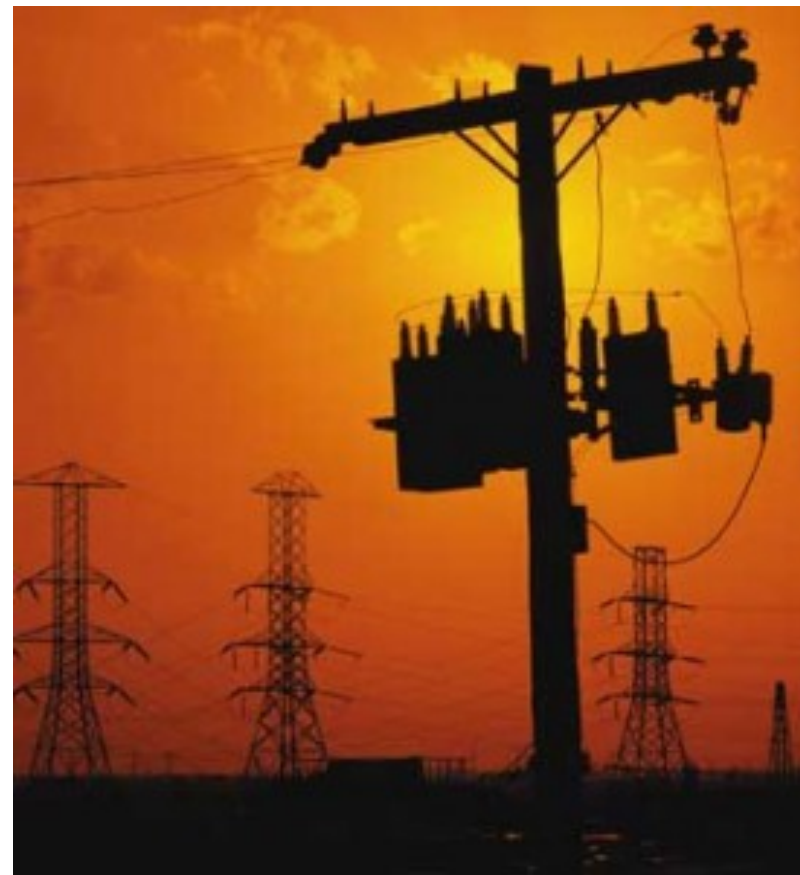




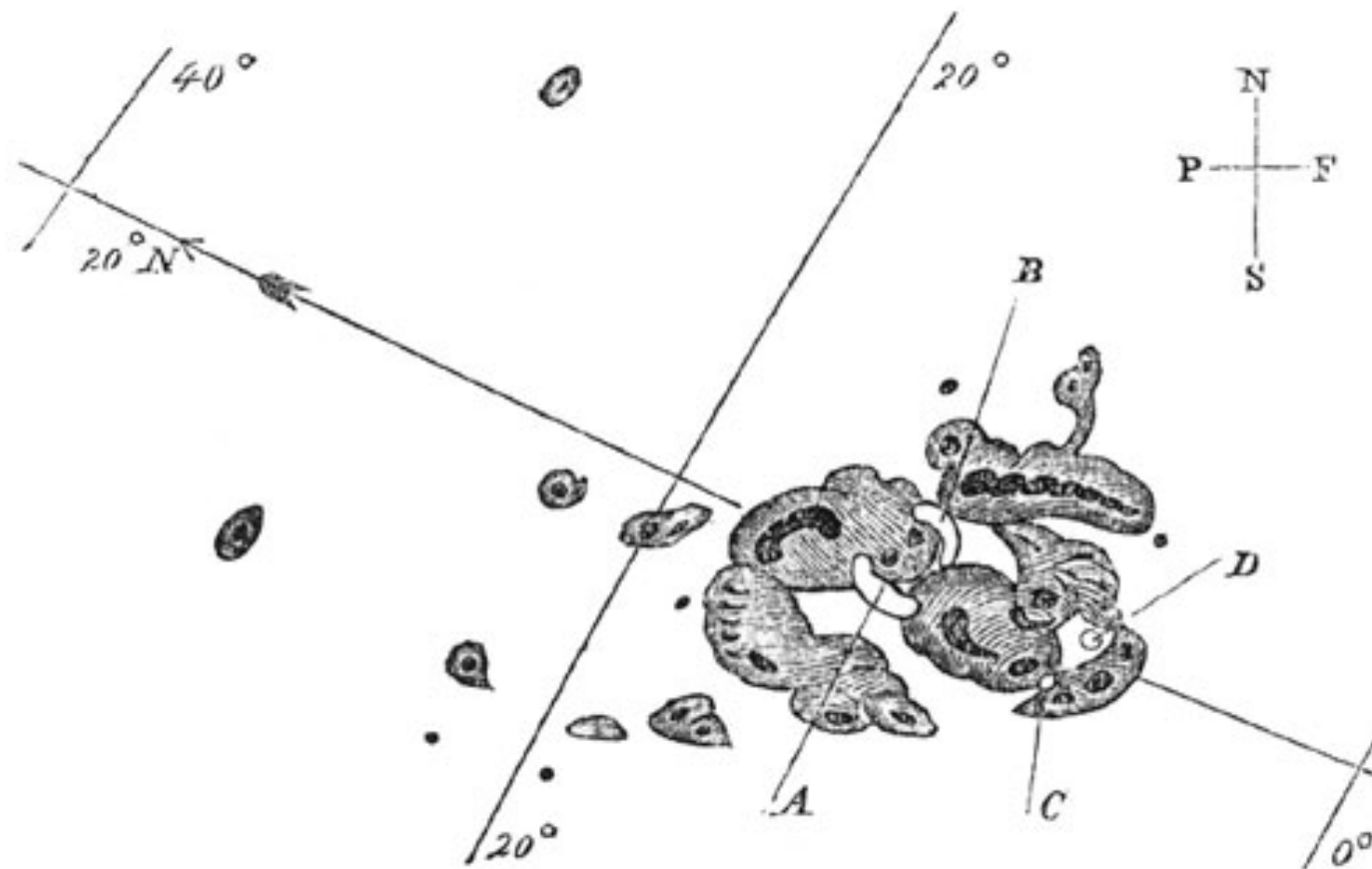
THE HABITABLE ZONE



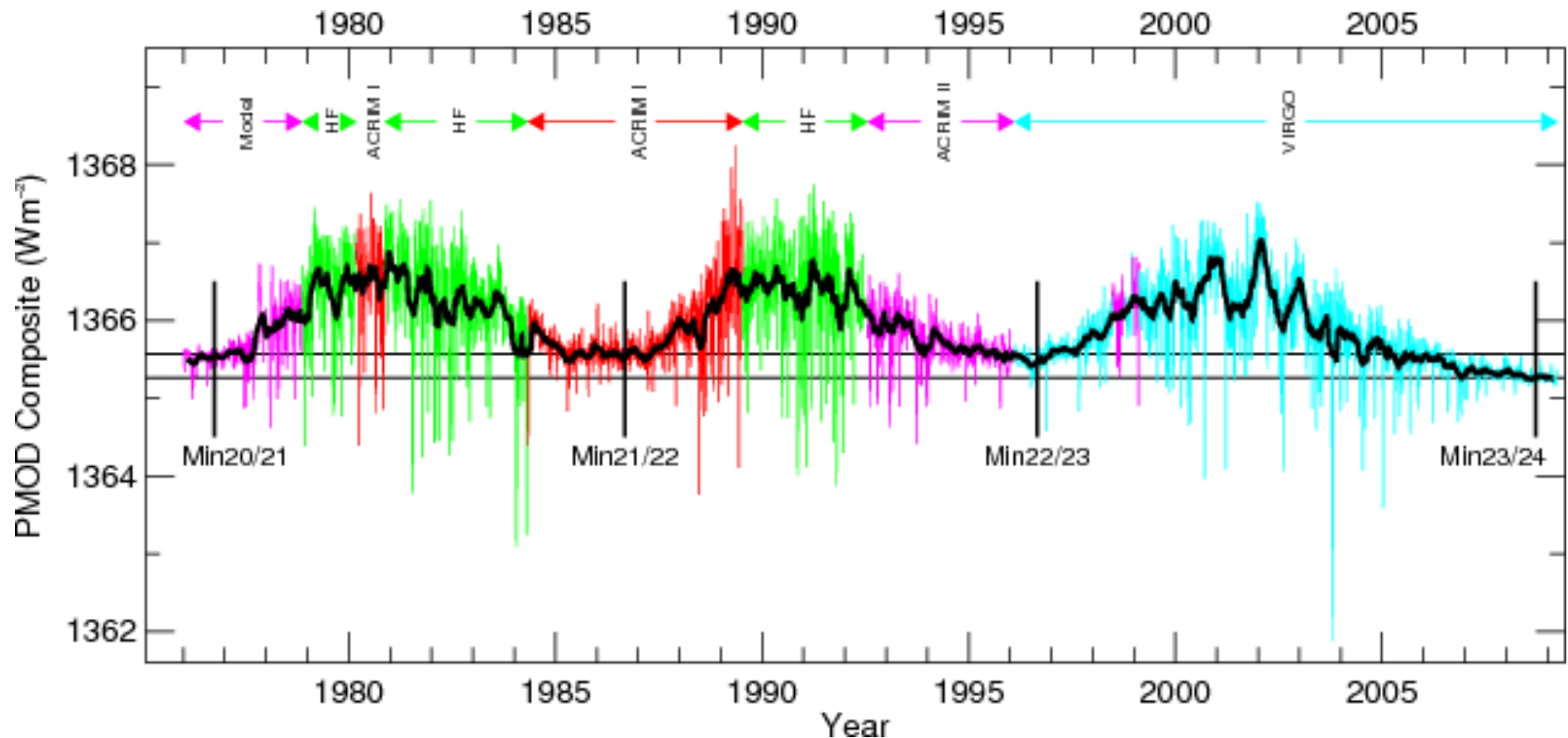
LIFE AND SUPER FLARES?



SOLAR STORM OF 1859



TOTAL SOLAR IRRADIANCE



SPOTS AND FACULAE

